



## 1 INTRODUCTION

Second Generation plasma accelerators are expected to be very demanding in terms of the required bunch length [1]. This is because the accelerated beam is required to be short with respect to the wavelength of the excited Langmuir plasma wave in order to maintain high beam quality and small energy spread. Since the anticipated wavelength ranges from 100 to 300  $\mu\text{m}$ , 1.5 to 15  $\mu\text{m}$  long bunches (rms) are required, with a bunch population of the order of  $10^8$  particles and a good emittance, namely less than 10 mm·mrad rms normalized in order to achieve the correct beam matching into the plasma channel (about 100  $\mu\text{m}$  wide).

Among the photo-cathode based injectors [2] the pulsed photo-diode [3] seems a good candidate to achieve very short bunches, mainly because of the high field gradient that can be applied on the photocathode surface, in excess of 1 GV/m. It is also attractive for its compactness and simplicity. The energy of the diode is typically low (e.g. 1-2 MeV) compared to rf guns. We will show how this low energy can be used to advantage since it allows for longitudinal bunch compression in the plasma that is not possible at higher energies.

The basic idea of the scheme described in this paper is for the bunch to undergo one quarter of a synchrotron oscillation in the bucket of the plasma wave, with injection on the minimum of the bucket close to the separatrix (zero acceleration phase) and extraction at the resonant energy  $\gamma_r$  just at the median line of the bucket (maximum acceleration). This phase oscillation in the bucket performs a bunching while it increases the absolute energy spread. Later the relative  $\Delta\gamma/\gamma$  is damped away. It will be shown that the final beam is fully consistent with the requirements on bunch length for a 2<sup>nd</sup> generation plasma accelerator [1] even though the injected beam is not (i.e. it is longer than the requirement). Such a compression mechanism can in principle be exploited even with a different injector, e.g. a radio-frequency gun. However, one should prove the ability of RF guns to produce 15  $\mu\text{m}$  long bunches at 24 pC of charge at energies of a few MeV ( $< 3$ ), so as to exploit the compression up to its maximum efficiency. In this paper we explore the use of a pulsed photo-diode for the simplicity and compactness of the apparatus, which allows a very short drift in between the diode and the plasma channel, minimizing in this way the de-bunching effect due to space charge.

It is worthwhile to mention that the idea to use a plasma wave to compress and/or modulate the density of an electron beam is not new: the plasma klystron concept, presented in ref. 9, is actually based on this idea. While the plasma klystron induces a density modulation on a beam which is much longer than the plasma wavelength [9], producing in this way a train of bunchlets, the system presented in this paper is expected to produce a single bunch shorter than the plasma wavelength.

In the second section of this paper we present a discussion of the beam dynamics in the diode and the drift to the plasma accelerator, with emphasis on how to transport the beam with minimum degradation of its quality (in particular the rms bunch length and energy spread). The beam dynamics modeling is based on a time dependent space charge code, HOMDYN [4], recently developed in the framework of RF photoinjectors. The code allows one to scan quickly over the parameter space, taking into account at the same time the emittance behavior and the debunching effect due to the longitudinal space charge field of the electron bunch. The model underlying the code is summarized in section 3, which presents also the results from the simulations, with particular concern to the adiabatic compression effect occurring when the beam

is injected at zero phase (no acceleration). Section 4 describes a possible method to control the time jitter between the HV pulse in the diode and the laser driving the plasma wave.

## 2 THE PULSED POTO-DIODE: A COMPACT INJECTOR SUITABLE FOR SHORT ELECTRON BUNCH GENERATION

The pulsed photo-diode is essentially an accelerating gap terminating a coaxial transmission line where a short (few ns) high voltage pulse (1-2 MV) is applied. The system basically consists of three components: a low voltage pulse generator (with a DC source at 25 kV), a Tesla transformer and a high voltage transmission line with SF<sub>6</sub> switches to sharpen the rise and fall times of the HV pulse.

Due to the short time duration of the pulse and the short gap of the diode (1-2 mm), it has been experimentally demonstrated [3] that it is possible to hold such high voltage pulses without break-down phenomena: very high field gradients, in excess of 1 GV/m, have been successfully applied at the photocathode surface. The high voltage pulse can be synchronized within 150 ps to an external laser (this will be later discussed in further details), so that the device can be operated as a DC photoinjector: a metallic photocathode hit by the laser emits photo-electrons during the laser pulse time duration. In this case the high voltage DC pulsed electric field plays the role of RF high gradient fields in RF guns. The electron bunch extracted from the diode is easily split from the laser beam illuminating the cathode in many ways: as an example one can illuminate the photocathode at an angle (60°-70°) as usually done in S-band RF guns[2], with proper correction of the laser wave fronts to avoid a tilt between them and the cathode plane (this would bring to an undesirable lengthening of the cathode emission time with respect to the laser pulse duration).

Because of such a strong field one can generate electron bunches at the cathode and accelerate them rapidly up to relativistic velocities (1-2 MeV). This should be done quickly, to freeze the space charge forces. Of particular concern is the longitudinal force that tends to introduce a bunch lengthening that would be detrimental to the quality of the beam. In view of the need for bunches no longer than 10 μm, and the fact that the cathode spot size is larger than 100 μm, one has to operate the beam in the surface charge regime typical of high aspect ratio bunches that look like thin pancakes. In this regime [5] the longitudinal space charge field scales like the inverse square of the bunch radius and is very weakly dependent on the bunch length.

Equation 1 shows a first order formula [5], giving the final electron bunch length  $\sigma_z$  (rms value at the diode exit) as a function of various parameters. These are the incident laser pulse length  $\sigma_l$ , the laser spot size at the cathode  $\sigma$ , the normalized field gradient  $\gamma' \equiv \frac{eE_0}{mc^2}$  (where  $E_0$  is the field gradient at the cathode) and the nominal beam peak current  $I_p$ .

$$\frac{\sigma_z}{\sigma_{las}} = \frac{I_p}{I} = 1 + \Delta_{sc} , \Delta_{sc} = \frac{I_p}{I_A(\gamma\sigma)} f(A_i, \gamma) \quad (1)$$

where  $\Delta_{sc}$  is the space charge debunching factor ( $I_A = 17$  kA). For high aspect ratios  $A_i = \frac{\sigma}{\sigma_l}$ , as typical of cases under discussion here, and final  $\gamma$  at the exit of the diode larger than 5, the factor  $f(A_i, \gamma)$  can be well approximated by  $f \approx A_i/3 - \sqrt{A_i}/80 - A_i^{1/4}/360$  (as far as  $1 < A_i < 100$  ;

the limit of  $f(A, \gamma)$  for very large A is  $\ln(2)$ .

In the drift following the diode gap one should expect a further debunching produced by the space charge induced energy spread, namely  $\frac{\Delta L}{L} = \frac{I_p \gamma' \sigma^2}{I_p \gamma'^2 \sigma^2}$ : this effect can be even larger than in the diode, since the bunch lengthening  $\gamma$  can be expressed, at first order, by  $\Delta L = \frac{I_p \gamma' \sigma^2}{\gamma^2}$ . According to these scaling laws one should, for a given desired peak current  $I_p$  (or for a given bunch length and charge), try to maximize the field gradient  $\gamma'$  and the cathode spot size  $\sigma$  (which is limited anyway by the anode aperture). Minimizing the drift length is also crucial.

As a particular example, consider a laser pulse of length  $\sigma_l = 12$  fs ( $4 \mu\text{m}$ ), spot size  $\sigma = 300 \mu\text{m}$ , diode gap 2 mm and field gradient at the photocathode 1.3 GV/m (so that  $\gamma=6$  at the diode exit), with a bunch charge of 24 pC ( $1.5 \cdot 10^8$  electrons,  $I_p = 600$  A). This leads to a predicted space charge debunching in the diode that is quite modest,  $\Delta_{SC} = 4.2 \%$ . The induced energy spread  $\frac{\Delta L}{L} = 0.05 \%$ , gives a further debunching  $\Delta L = 8 \mu\text{m}$  at the end of the 26 cm long drift space to the plasma channel. It will be shown in the final section that the simulations agree remarkably well with these analytical predictions. This points out the need of short laser pulses and high field gradients to keep the bunch length within the demands of the plasma accelerator.

The transverse beam dynamics sets up some other constraints dealing with the matching of the beam into the plasma wave. The most important issue is the minimum drift length achievable compatibly with the need to apply some focusing to obtain the correct matching. In fact, the diode, having a flat cathode is equivalent to having a defocusing lens. A curved cathode should be avoided since it leads to bunch lengthening due to electron trajectories of varying length emerging from various points on the curved cathode [6]. The rms beam divergence at the exit is predicted to be

$$\sigma' = \frac{\sigma_{cat}}{2d} F(\gamma'd) + \frac{\pi I_p}{12 I_A \sigma \gamma'} \quad (2)$$

Here  $d$  is the diode gap length and the expression for the factor  $F(v)$  is reported in the Appendix.  $F(v)$  is very close to 1 for our case of interest, where  $v = \gamma'd \gg 1$ .

According to eq.2 we conclude that the diode applies a serious defocusing kick to the beam. The source is the first term in the r.h.s. of eq.2, which is due to the radial field lines of the exit aperture close to the cathode. This term is much larger than the space charge kick (second term in the r.h.s): in fact for the parameters listed above we obtain  $\sigma' = 75 \text{ mrad} + 2 \text{ mrad}$ . In order to overcome such a high beam divergence at the exit of the diode, we place a solenoid lens at 11 cm from the cathode, set at 2.5 kGauss peak field. The solenoid must focus down the beam into the plasma wave accelerator, which requires a beam spot size of about  $50 \mu\text{m}$ . The simulation results are shown at the end of the next section.

### 3 THE HOMDYN MODEL AND ITS ENHANCEMENT TO TREAT ACCELERATION IN PLAMA WAVES

Time dependent space charge effects play a crucial role in the beam dynamics of high brightness injectors. A fast running code (HOMDYN) has been developed to deal with the evolution of high charge, not fully relativistic multi-bunch beams in RF fields of an accelerating cavity, taking into account the field induced by the beam in the fundamental and higher order modes, and the variation of bunch sizes due to both the RF fields and space charge. Such a code is suitable also for the present application where instead of an rf cavity we have an accelerating gap followed by a plasma channel.

In modeling the plasma wave we include the fields of an externally-driven linear plasma wave, but neglect the self-generated wakefields due to the beam loading of the plasma wake. This is justified providing the beam load is not too large [7]; namely when the electron number  $N$  is such that:

$$eN \ll (100 \text{ pC}) E[\text{GeV}/m] \frac{\text{wave area}}{[100 \text{ }\mu\text{m}]^2}$$

We review in this section the main features of the model, with some modifications added specifically for the case under study.

The basic approximation in the description of beam dynamics lays in the assumption that each bunch is described by a uniform charged cylinder, whose length and radius can vary under a self-similar time evolution while keeping a uniform charge distribution inside the bunch. By slicing the bunch in an array of cylinders (Multi-Slices Approximation, see Fig. 1), each one subject to the local fields, one obtains also the energy spread and the emittance degradation due to phase correlation of RF and space charge effects.

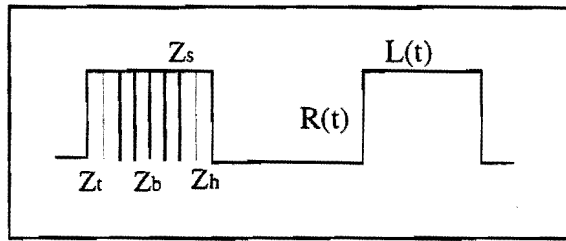


**FIG. 1:** Electron bunch as modeled by the code HOMDYN to calculate the space charge field: uniform cylindrical distribution represented by  $N$  slices. See text for definitions of the slice coordinates  $z_s$ , bunch sizes  $R(t), L(t)$  and bunch coordinates  $z_t, z_b, z_h$ .

The longitudinal space charge fields on axis at a distance  $\zeta_s = z_s - z_t$  of the  $s^{\text{th}}$  slice from the bunch tail located at  $z_t$ , is given by [6]:

$$E_r^{sc}(\zeta_s) = \frac{Q}{2\pi\epsilon_0 R_s^2} H(\zeta_s, A_{r,s})$$

where

$$H(\zeta_s, A_{r,s}) = \sqrt{(1 - \zeta_s/L)^2 + A_{r,s}^2} - \sqrt{(\zeta_s/L)^2 + A_{r,s}^2} - (1 - 2\zeta_s/L)$$

and  $Q$  is the bunch charge,  $L$  the bunch length,  $R_s$  the slice radius and  $A_{r,s} \equiv R_s/(\gamma_s L)$  is the

slice rest frame aspect ratio.

The radial space charge fields (linear component) of the same slice, is given by:

$$E_r^{sc}(\zeta_s) = \frac{Q}{4\pi\epsilon_0 R_s L} G(\zeta_s, A_{r,s})$$

where

$$G(\zeta_s, A_{r,s}) = \frac{1 - \zeta_s/L}{\sqrt{(1 - \zeta_s/L)^2 + A_{r,s}^2}} + \frac{\zeta_s/L}{\sqrt{(\zeta_s/L)^2 + A_{r,s}^2}}$$

The plasma longitudinal and transverse (linear component) fields are:

$$E_z^{pl}(z_s) = E_o \sin(\omega_p t - k_p z_s + \psi_o) \left(1 - \frac{R_s^2}{a^2}\right)$$

and

$$E_r^{pl}(z_s) = -\frac{2E_o R_s}{a^2 k_p} \cos(\omega_p t - k_p z_s + \psi_o)$$

The equations for the longitudinal motion for each slice are:

$$\dot{z}_s = \beta_s c$$

$$\dot{\beta}_s = \frac{e}{m_o c \gamma_s^3} (E_z(z_s, t) + E_z^{sc}(\zeta_s, t) + E_z^{pl}(z_s, t))$$

The evolution of each slice radius  $R_s$  is described in the time-domain according to an envelope equation, including damping due to acceleration (second term), solenoid focusing (third), RF-focusing (fourth) plasma focusing (fifth), space charge effects (sixth), image charges from the cathode surface (seventh): and thermal emittance pressure (eighth):

$$\begin{aligned} \ddot{R}_s + \beta_s \gamma_s^2 \dot{\beta}_s \dot{R}_s + (K_s^{sol} + K_s^{rf} + K_s^{pl}) R_s &= \\ = \frac{2c^2 k_p}{R_s \beta_s} \left( \frac{G(\zeta_s, A_r)}{\gamma_s^3} - (1 + \beta_s^2) \frac{G(\xi_s, A_r)}{\gamma_s} \right) + \left( \frac{4\epsilon_n^{th} c}{\gamma_s} \right)^2 \frac{1}{R_s^3} \end{aligned}$$

where the dots indicate the derivation with respect to time and

$$K_s^{sol} = \left( \frac{eB_z(z_s)}{2m_o \gamma_s} \right)^2 \text{ is the solenoid focusing gradient,}$$

$$K_s^{rf} = \frac{e}{2\gamma_s m_o} \left( \frac{\partial E_z}{\partial z} + \frac{\beta_s}{c} \frac{\partial E_z}{\partial t} \right) \text{ is the RF focusing gradient expressed through the linear}$$

expansion off-axis of the accelerating field  $E_z = E_z(0, z, t)$ ,

$$K_s^{pl} = \frac{2eE_o}{\gamma_s m_o a^2 k_p} \cos(\omega_p t - k_p z_s + \psi_o) \text{ is the plasma focusing gradient,}$$

$$k_p = \frac{I(\zeta_s)}{2I_o} \text{ is the beam perveance and } \epsilon_n^{th} \text{ is the rms normalized thermal beam emittance.}$$

In order to evaluate the degradation of the rms emittance produced by longitudinal

correlation in space charge and transverse external forces, we use the following expression for the correlated emittance:  $\epsilon_n^{cor} = \frac{1}{4} \sqrt{\langle R_s^2 \rangle \langle (\beta \gamma R_s')^2 \rangle - \langle R_s \beta \gamma R_s' \rangle^2}$  where  $R_s' = \frac{d}{dz} R_s$  and the average  $\langle \rangle = \frac{1}{N} \sum_{s=1}^N$  is performed over the N slices. The total rms emittance will be given by a quadratic summation of the thermal emittance and the correlated emittance:  $\epsilon_n = \sqrt{(\epsilon_n^{th})^2 + (\epsilon_n^{cor})^2}$ .

The simulations of the system have been carried out choosing the following set of parameters: the diode is driven by a 1.3 MV HV pulse applied to a 2 mm gap, while the laser pulse hitting the photocathode is 40 fs long (assumed to be flat top in time, note that this is equivalent to a 12 fs rms laser pulse length) and is focused down to a 0.6 mm spot size (hard edge radius of a uniform radial intensity profile), extracting 24 pC of charge. In order to take under control the large defocusing kick received by crossing the anode hole (as discussed in Sect.1) we apply a focusing solenoid lens located 11 cm from the cathode with a field amplitude of 2.5 kGauss (peak field on axis). The plasma wave is assumed to have a plasma wavelength of 300 microns, radius  $a=100$  microns, starting 26.7 cm from the cathode and extending through 10 cm with an accelerating gradient of 3 GV/m. The resonant *gamma* of the wave is taken to be  $\gamma_r = 400$ .

The beam kinetic energy (dotted line), the rms energy spread (dashed line) and the rms bunch length (solid line) are shown in Fig.2 for the case of injection at zero acceleration phase (i.e.  $\psi_o = 0^0$ ) into the plasma wave. The injection energy is 2.45 MeV, with a bunch length of 3.5 microns at the diode exit and 15.5 microns at the end of the drift to the plasma wave – bunch lengthening caused by the longitudinal space charge field. The bunching action of the plasma wave, effective at a proper injection phase of 0 degrees (no acceleration), causes a reduction of the bunch length in opposition to the space charge effect, with a final equilibrium bunch length of 3 microns with an energy spread of 6%. Matching the beam into the strong focusing channel of the plasma wave is quite critical. An example is shown in figure 3, indicating the rms radius (solid line) and the rms normalized emittance (dashed line). The beam is blown up radially to 8 mm rms radius in the center of the solenoid (11 cm from the cathode) and focused down to 50 microns into the plasma wave.

It is interesting to notice that an injection at 60 degrees assures maximum acceleration up to 292 MeV exit energy but no bunching effect, as shown in figure 4, where the final bunch length is 17 microns at an energy spread of 12%.

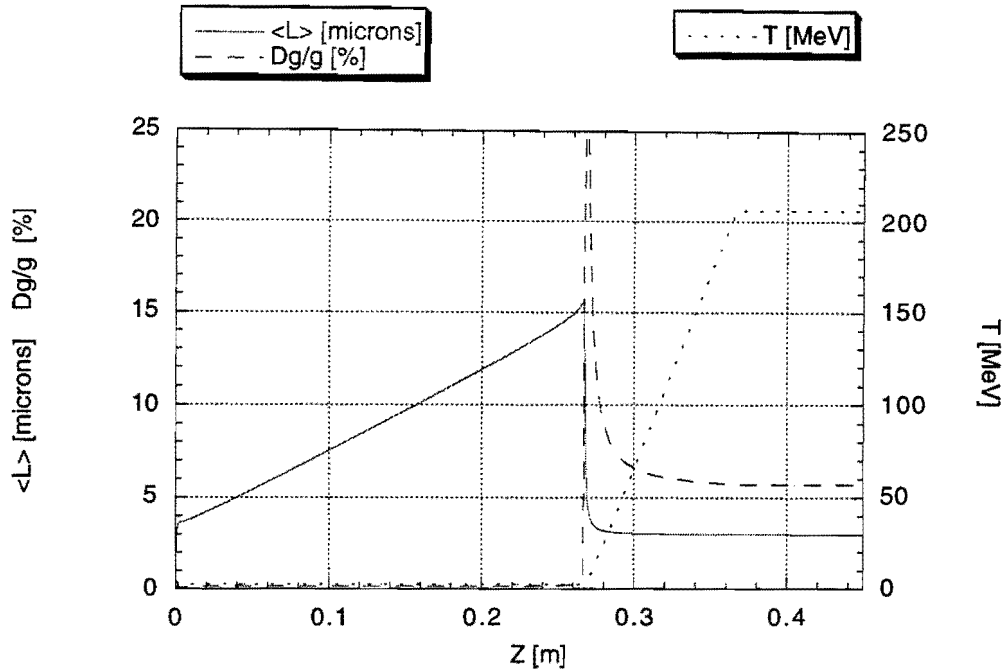


**FIG. 2:** Longitudinal dynamics at  $0^\circ$  injection phase (no acceleration). Solid line (left scale) represents the rms electron bunch length. Dotted line (right scale) represents the bunch average energy and dashed line (left scale) represents the rms energy spread.

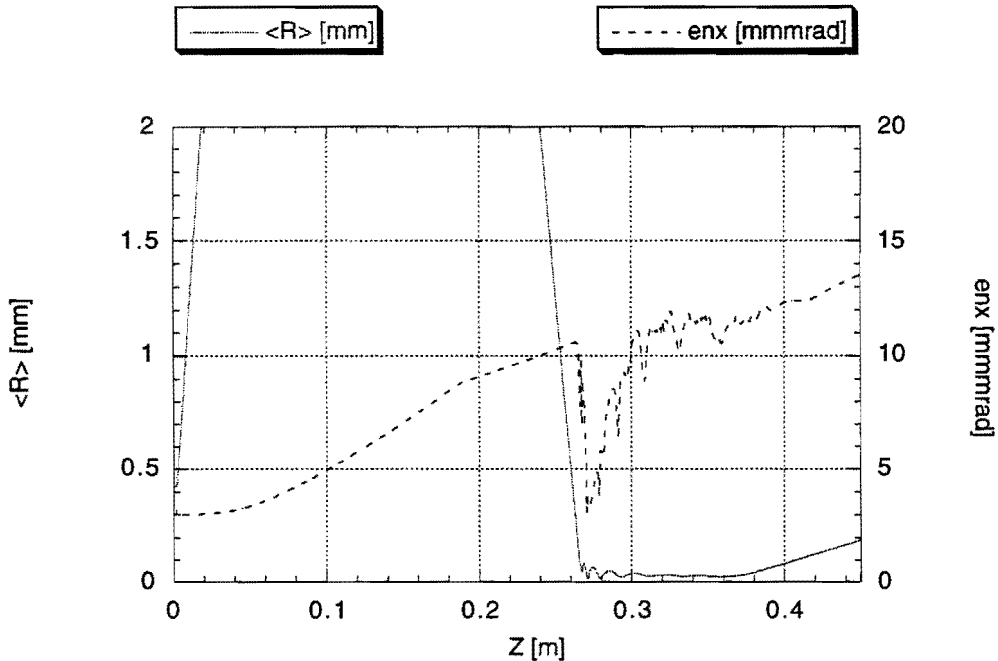


**FIG. 3:** Transverse dynamics at  $0^\circ$  injection phase (no acceleration). Solid line (left scale) represents the rms electron bunch radius: the scale is set so to show the matching into the plasma wave at  $z=0.267$  (maximum rms radius is 8 mm at  $z=0.11$ ). Dashed line (right scale) represents the rms normalized transverse emittance.

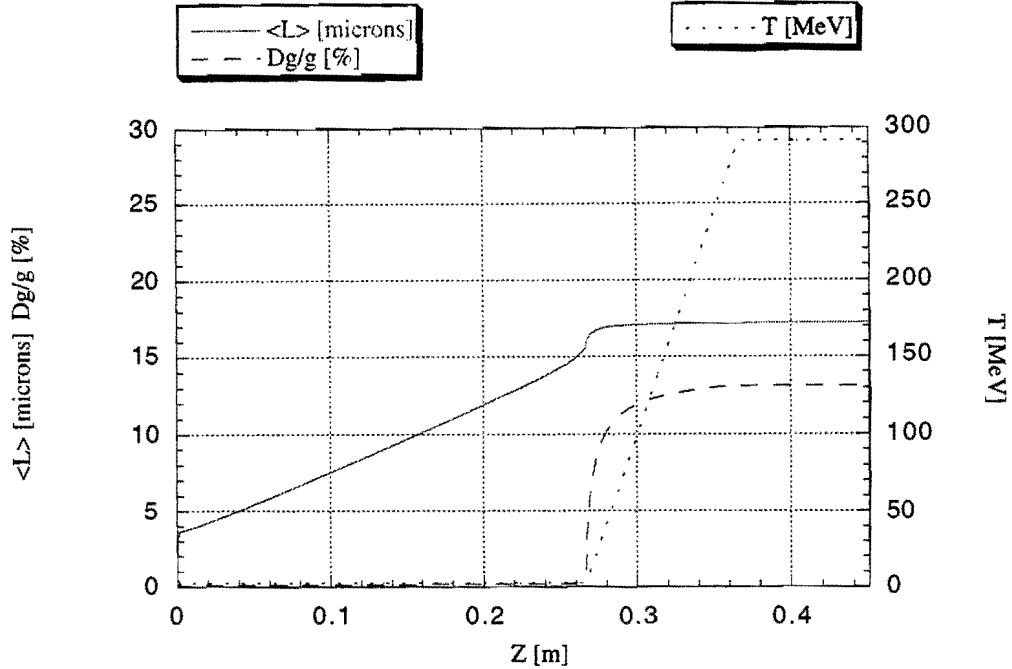


**FIG. 4:** Longitudinal dynamics at  $60^\circ$  injection phase (maximum acceleration). Solid line (left scale) represents the rms electron bunch length. Dashed line (right scale) represents the rms energy spread.

#### 4 CONTROL OF THE TIME JITTER BETWEEN THE PLASMA WAVE AND THE HV PULSE

The acceleration in the plasma wave changes very rapidly with the injection phase of the electron bunch. In order to get a consistent acceleration and small energy jitter (pulse-to-pulse) we must control the timing of the injection with unprecedented precision.

The attainment of such stability by synchronization of lasers is hopeless. Therefore we assume that a single laser controls the timing of both photocathode illumination and plasma wake generation. This still requires attention to minute details in maintaining constant laser path lengths in the system. That includes highly stable optical component support, covered and temperature controlled light pathways and similar, well-known optical-transport practices. This leaves us with the main challenge being the variation of the electron time-of-arrival.

The variation in the electron timing is due to the shot-to-shot variation in the accelerating potential. The pulsed diode waveform is timed by spark gaps. The triggering of a spark gap is a statistical process of creating an avalanche. The use of special liquids in the spark gap, laser triggering and advanced geometry can reduce the jitter to under one nanosecond. Since the pulse can not be made absolutely uniform over the entire waveform, which is approximately flat-top over one nanosecond, we have to deal with pulse to pulse acceleration voltage jitter of a few percent. Thus a timing jitter is generated by the time of flight dependence on the voltage.

The time jitter per a fraction of the accelerating voltage jitter is given as the sum of two terms, the jitter in the diode and the jitter in the drift space past the diode.

The first is given as  $1/(c\gamma')$ , the other as  $(L_{\text{drift}}/c)(2\gamma'd/(2+\gamma'd))(2\gamma'd+\gamma'^2d^2)^{-1/2}$ . For typical values of  $d=0.002$  m, and  $\gamma'd=2$  we see that the timing jitter in the diode itself is of the

order of 30 fs per percent amplitude jitter. In a drift of 0.3 m past the diode the jitter is about 3 ps per percent.

In other words, a pulse-to-pulse correction of the order of a few picoseconds is necessary to maintain the electron bunch and the plasma wave in synchronism.

We propose to correct this jitter by a feed-forward scheme. The principle is quite simple: A pick-up electrode inserted in the high-voltage transmission line will measure the voltage of the diode. The voltage of the pulse is so high that even a weakly coupled probe will generate enough signal to eliminate the need for an amplifier.

The electric signal will change the path length of the laser propagating towards the photocathode. The magnitude of the change is adjusted so that a compensation of the jitter is accomplished.

To make this possible it is necessary to design the path length of the high voltage pulse from the measurement point to the cathode to allow enough delay to enable the feed forward adjustment. The laser pulse must arrive at the cathode at the same time that the part of the pulse that produced the path length change arrives.

The laser variable delay line will be composed of optically active material that changes the index of refraction upon the application of an electrical field. The optical path length of a laser beam in a medium changes dramatically if the medium is highly dispersive at the laser wavelength and the molecular levels contributing to the dispersion is shifted. Such an energy level shift can be accomplished either by applying an electric field or even using the electric field associated with the laser by invoking the Stark effect. Appropriate choice of the medium and the magnitude of the field may result in the required path length. The major draw back of this technique would be the corresponding change in the absorption coefficient. The transport loss of the laser will then be a function of the field, which needs to be corrected.

The photocathode laser starts as an IR laser, which is, usually, multiplied to the UV. The calculations that we will present to establish the principle correspond to the effect in ammonia, at a wavelength of 10.6  $\mu\text{m}$ , where data has been available. More research is necessary to identify a proper material and wavelength for UV operation.

Stark shifting of a vibrational-rotational line of ammonia has been done for spectroscopic applications [8]. The ammonia lines have been shifted in and out of resonance by applying moderate electric fields. The fields necessary to tune through resonance varied depending on the line in question. A voltage as low as 30 V over two mm gap (field of 15 kV/m) is sufficient for some lines. This introduces a large change in the refractive index and hence the path length of the laser to correct for the jitter. Based on data taken from Ref. 8, the produced change in the refractive index  $\Delta n_r$  as the resonance is shifted between 9.503  $\mu\text{m}$  and 9.443  $\mu\text{m}$  is 2.928-0.419=2.509. Therefore, the length required to change the path length by 1 ps is  $L = 1 \times 10^{-12} \text{ s} \times 3 \times 10^{10} \text{ cm/s} / 2.509 = 120 \mu\text{m}$

The imaginary part of the refractive index that affects the absorption changes from 1.459 to 2 in this change of wavelength.

Incidentally, ammonia has also a resonance line in UV at 200 nm where the change in the refractive index  $\Delta n_r$  is 0.3. If this resonance is used, the required length would be 1 mm. However, it is most likely that there are other material candidates.

Concerning the possible breakdown of the laser transported through the cell, it should be

noted that the necessary power is not very high. With the high electric field on the cathode and using clean copper surfaces. A quantum efficiency of 0.05% was obtained at 100 MV/m, and at the diode's operating field of 1 GV/m the expected quantum efficiency is 0.5%. At this quantum efficiency the necessary laser energy is about 24 nJ, or a power of 1 MW. This is not expected to result in breakdown problems over a spot size of about 1 mm.

This example is given just as a demonstration of principle and more work is necessary to produce a practical working device. Besides the identification of the optimal resonant Stark effect material, there are some other concerns to be addressed. These are listed below as pointers for further research.

The calculation above was made with solid ammonia, where the number density is  $\sim 4$  orders of magnitude larger than the atmospheric gas. High-pressure ammonia gas may be used, but since the refractive index is directly proportional to the electron density, the length of the ammonia cell would have to be increased.

What would be the optical quality of this ammonia column, as solid or gas? Can the laser beam quality be maintained after passage through this cell?

Stark shift measurements have been done only in gaseous ammonia. Are the results valid in solid ammonia?

How does broadening due to pressure and laser intensity affect the results?

Can the ammonia hold off the large background field of the pulse (besides the ripple used to affect the shift?)

The necessary response time is commensurate with the rate of change of the voltage on the pulsed diode, which is of the order of tens of one hundred picoseconds. Is the response time of the molecule to the applied field sufficiently fast?

Finally, the change in absorption needs to be calculated and corrected for.

## 5 CONCLUSIONS

We have shown by means of a preliminary analysis that a proper injection (by using a specific beam energy and phase) into a plasma wave can relax the demands for beam quality, in particular the maximum bunch length and energy spread acceptable at injection, to meet the requirements of 2<sup>nd</sup> generation plasma accelerators. We found great advantages in the use of pulsed photodiodes as injectors and beam sources, mainly because of their compactness and the very high gradient achievable at the photocathode surface.

Other issues have to be more carefully investigated besides what has been done for this analysis: wake fields effects in the plasma wave (i.e. beam loading), spatial variation of the plasma wave accelerating gradient due to laser envelope, multi-particle effects not addressable with the use of HOMDYN. These are topics for future investigations.

## 6 ACKNOWLEDGEMENT

We thank Triveni Srinivasan-Rao for stimulating discussions on optical feedback mechanisms.

## 7 APPENDIX

We assume a first order linear on-axis expansion for the static accelerating field

$$\begin{cases} E_z = E_0 f(x) \\ E_r = -\frac{E_0 r}{2d} f'(x) \end{cases} ; x = \frac{z}{d}, f' = \frac{df}{dx}$$

where the field form factor on-axis is specified generically by the normalized function  $f(x)$ , such that  $f(0) = 1$  and  $f \xrightarrow{x \rightarrow \infty} 0$ . The beam normalized energy at the gap exit will be given by

$$\gamma = 1 + v \int_0^{\infty} f dx$$

where the dimensionless quantity  $v = \frac{eE_0 d}{mc^2}$  represents an effective normalized gap voltage across the gap of length  $d$ . Recalling that the transverse momentum change through the gap is  $\Delta p_r = \int_0^{\infty} eE_r dt$ , and  $\frac{d}{dt} = \frac{d}{\beta c} \frac{d}{dx}$  ( $\beta = \sqrt{1 - \frac{1}{\gamma^2}}$ ), the beam rms divergence at the gap exit, defined by  $\sigma' = \frac{\Delta p_r(r = \sigma)}{mc\beta\gamma}$  under the assumptions of straight electron trajectories through the gap and laminar beam, will be given by

$$\sigma' = \frac{\sigma}{2d} F(v)$$

where

$$F(v) = -v \int_0^{\infty} \frac{f'(x)}{\sqrt{1 - \left(1 + v \int_0^x f(y) dy\right)^2}} dx \left/ \sqrt{\left(1 + v \int_0^{\infty} f(x) dx\right)^2 - 1}\right.$$

The form factor  $F(v)$  has a relativistic limit, *i.e.* at  $v \gg 1$ , given by  $F \xrightarrow{v \rightarrow \infty} F_{\infty} = \frac{1}{\int_0^{\infty} f(x) dx}$  (typically  $F_{\infty} = O(1)$ , implying  $\sigma'(v \gg 1) = \frac{\sigma}{2d}$ ), while the limit

at very small  $v$  is  $F \xrightarrow{v \rightarrow 0} F_0 = \frac{1}{2} \int_0^{\infty} \frac{f'(x)}{\sqrt{\int_0^x f(y) dy}} dx$ , which is again a quantity typically of the

order of 1 for a well behaved function  $f(x)$  as previously specified (implying  $\sigma'(v \ll 1) = \frac{\sigma}{4d}$ ).

The behavior of the form factor  $F(v)$  corresponding to a gaussian electric field distribution on-axis, *i.e.* for  $f(x) = e^{-x^2/2}$ , which is very close to that of a flat cathode-flat anode geometry for the diode gap, is plotted in Fig.5 versus  $v$ .

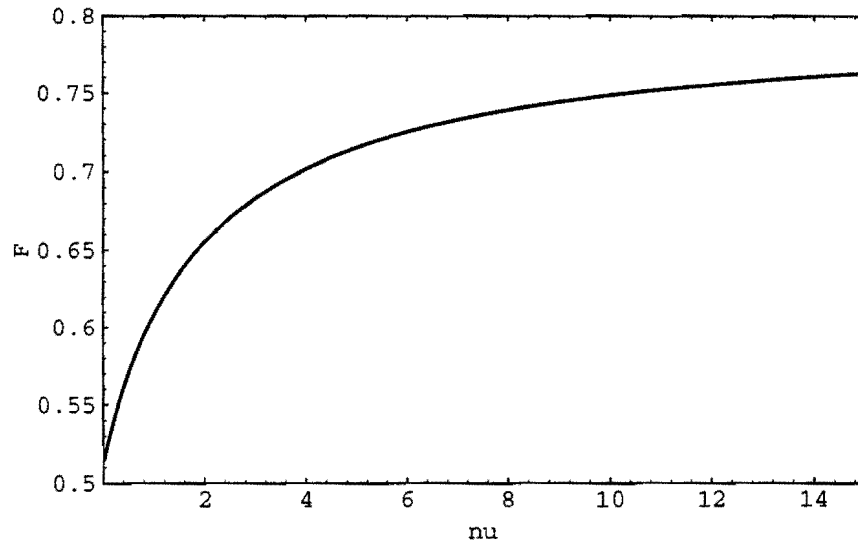


**FIG. 5:** Form factor  $F(v)$  plotted as a function of  $v$  for the case  $f(x) = e^{-x^2/2}$ , i.e. a gaussian electric field distribution on axis through the diode gap.

## 8 REFERENCES

- (1) C. Clayton, L. Serafini, *IEEE Trans. on Plasma Science* **24**, No.2, 1996, p.400
- (2) C. Travier, *Particle Accelerators* **36** (1991), p.33
- (3) T. Srinivasan-Rao *et al.*, *AIP CP* **398**, 249 (1997)
- (4) M. Ferrario *et al.*, *Particle Accelerators* **52**, 1996, p.1
- (5) L. Serafini, *AIP CP* **413**, 1997, p.321
- (6) L. Serafini, *IEEE Trans. on Plasma Science* **24**, No.2, 1996, p.421
- (7) T. Katsouleas *et al.*, *Part. Accel.* **21**, 1987, p.81
- (8) J. V. Martonchik *et al.*, *Appl. Optics* **24**, No. 4, 1984, p. 541
- (9) T. Katsouleas *et al.*, *IEEE Trans. on Plasma Science* **24**, No.2, 1996, p.443